

# Compromised DNA Repair and Signalling in Human Granulocytes

Viviane Ponath Daniel Heylmann Tobias Haak Kevin Woods Huong Becker  
Bernd Kaina

Department of Toxicology, University Medical Center, Mainz, Germany

## Keywords

DNA repair · Neutrophilic granulocytes · DNA damage ·  
Cell death · Immune cells

## Abstract

In previous studies, we showed impaired DNA repair in human monocytes. Here, we addressed the question of whether human neutrophilic granulocytes that arise from the same precursor as monocytes exhibit a similar phenotype and are impaired in repairing their DNA. We show that neutrophilic granulocytes isolated from peripheral blood display a lack of the same repair proteins that are missing in monocytes and do not show repair of their DNA when damaged by ionising radiation (IR) or chemical ROS. Contrary to T cells, we observed no decline in the number of single-strand breaks following  $\gamma$ -radiation. Also, granulocytes did not show  $\gamma$ H2AX foci formation while T cells and peripheral blood lymphocytes (PBL) responded. In comparison to PBL, XRCC1, PARP-1 and ligase III were not expressed and there was also no discernible signal for key damage response proteins ATM, ATR and DNA-PK $\text{CS}$  as well as  $\gamma$ H2AX in neutrophils. Time course and dose-response experiments confirmed the absence of

H2AX phosphorylation after radiation treatment although an accumulation of double-strand breaks was detected in the neutral Comet assay. Overall, the data indicate that terminally differentiated neutrophilic granulocytes in the peripheral blood display strong downregulation of DNA repair and DNA damage response factors, which should be taken into account if studies with whole peripheral blood containing granulocytes are performed, causing a significant intra-experimental variation in the cellular repair capacity.

© 2018 The Author(s)

Published by S. Karger AG, Basel

## Introduction

Polymorphonuclear neutrophilic granulocytes (neutrophils) are the most abundant leukocytes in the peripheral blood. They amount to 50–70% of leukocytes in humans, while in mice the frequency is much lower with 10–25% [1]. Granulocytes are essential for the innate immune reaction as they are responsible for the engulfment and destruction of invading pathogens. Their importance is highlighted by severe diseases where neutrophils are absent or dysfunctional, e.g. neutropenia, chronic granu-

lomatous disease and leukocyte adhesion deficiency [1, 2]. However, neutrophils also show destructive potential as observed in inflammatory diseases such as rheumatoid arthritis and chronic obstructive pulmonary disease [3–5]. Therefore, it is of great importance to maintain a healthy balance of neutrophil production and clearance. The number of neutrophils can be regulated at several stages, i.e. during granulopoiesis, the release from the bone marrow, the distribution of circulating and resting neutrophils as well as the half-life and subsequent clearance from the blood. Under normal conditions, approximately  $0.87 \times 10^9$  neutrophils/kg body weight are released each day from the bone marrow to the blood stream [1, 2]. The number increases under inflammatory conditions. The circulatory lifespan ranges from hours to a few days before neutrophils undergo apoptosis and are phagocytosed by macrophages and dendritic cells (DC) [3]. In the process of their maturation, several stages can be distinguished, namely myeloblast, promyeloblast, myelocyte, metamyelocyte, band cell and finally granulocyte. Mature neutrophils display the characteristic segmentation of the nucleus and prominent granules [3].

Neutrophils have an extensive defensive repertoire to fight infections. The phagocyte NADPH oxidase (NOX2) catalyses the production of superoxide radicals and its metabolite hydrogen peroxide can damage pathogens in the vicinity [6]. This so-called oxidative burst can also be observed in other phagocytes such as monocytes and macrophages [7–9]. The neutrophil extracellular traps (NET) represent another defensive mechanism [10–12]. They are web-like structures consisting of DNA, histones and anti-microbial factors, e.g. neutrophil elastase, lactoferrin and defensin peptides. NETs are exported to the extracellular space where they can immobilise and kill pathogens before they are phagocytosed by inflammatory macrophages. This phenomenon can also be observed *in vitro* after treatment with phorbol-12-myristate 13-acetate (PMA), lipopolysaccharide or ionophore. The successful formation of NETs requires, among others, a functional NADPH oxidase system. Although the mechanisms are not yet fully understood, data indicate that activated neutrophils respond with a high level of ROS, are programmed to undergo suicide and NETs are activated. The excessive ROS production of neutrophils raises the question of whether and how these cells are protected against ROS-induced DNA damage.

The myeloblast is not only the progenitor of neutrophilic granulocytes, but also of monocytes. In previous studies, we have shown that monocytes are impaired in DNA repair. They express at a very low (almost non-de-

tectable) level key proteins required for efficient DNA repair, i.e. XRCC1, PARP-1, ligase III $\alpha$  and DNA-PK $\text{CS}$ . This results in a low capacity of base excision repair (BER) and DNA double-strand break (DSB) repair, specifically in the non-homologous end-joining (NHEJ) pathway [13, 14]. Consequently, monocytes are susceptible to ionising radiation and oxidising and alkylating genotoxic agents, and undergo apoptosis at a higher level than macrophages and DC following DNA damage [14, 15]. This repair deficiency is abrogated if monocytes undergo cytokine-induced differentiation into macrophages or DC. Thus, monocyte-matured macrophages and DC re-express the relevant DNA repair proteins and therefore become resistant to genotoxins, including ionising radiation, chemical ROS and anticancer drugs [9, 13, 14]. Of note, T cells are repair competent similar to differentiated macrophages [16].

Since granulocytes and monocytes arise from the same precursor in the bone marrow [16], we wondered whether granulocytes exhibit the same DNA repair defective phenotype as monocytes. Therefore, in this study, we analysed granulocytes (the majority in the population is neutrophils) and compared them with T cells as to their expression of DNA recognition and repair factors, their DNA repair capacity after genotoxic insult and induction of cell death. We specifically focused on PARP-1, which is an NAD $^{+}$ -dependent enzyme which becomes activated upon DNA single- and double-strand breaks and catalyses the formation of poly(ADP-ribose), a biopolymer that binds to PARP-1 itself and other DNA repair factors. It recruits these factors to the site of damage and removes histones from the DNA, thus opening the DNA for repair. PARP-1 is also involved in alternative non-homologous end-joining (B-NHEJ), serving as a backup repair pathway to the canonical NHEJ [17]. Together with XRCC1 and ligase III it helps ligate DSBs, although this is considered to be an error-prone repair pathway. In contrast to PARP-1, XRCC1 has no enzyme activity. It is a scaffold protein involved in BER and alternative NHEJ and stabilises ligase III [18]. This ligase is involved in BER and religates nicked DNA. DNA-PK, ATM and ATR are kinases involved in the recognition of DSBs (DNA-PK $\text{CS}$ , ATM) and stalled replication forks (ATR). When activated, they phosphorylate a large number of downstream targets [19] and are involved in the regulation of DNA repair, apoptosis and other DNA damage response (DDR) endpoints [20]. Here, we show that these repair and DDR factors are lacking in terminally differentiated granulocytes in the peripheral blood.

## Material and Methods

### *Isolation of Granulocytes and PBL from Buffy Coats*

Human granulocytes and PBL were isolated from buffy coats supplied by the blood bank of the University Medical Center, Mainz. Granulocytes were isolated by the Optiprep density method as described previously [9]. Briefly, two solutions of different densities (solution A 1.077 g/mL and solution B 1.095 g/mL) were prepared from Optiprep (density 1.32 g/mL, Progen Biotechnik GmbH, Heidelberg, Germany) diluted in 0.85% NaCl, 1 mM EDTA, 20 mM HEPES, pH 7.4. Thereafter, 9 mL of blood were mixed with 1 mL of 6% dextran sulphate sodium salt (Sigma-Aldrich, Steinheim, Germany) dissolved in 0.85% NaCl buffer and incubated for 1 h at room temperature (RT) until a clear upper phase was visible. The upper phase was transferred into a fresh 15-mL tube on top of 4 mL of solution A in the middle and 4 mL of solution B at the bottom. The samples were centrifuged at 1,900 rpm for 30 min without brake. Two rings of cells were visible and the lower ring containing the granulocytes was collected. The cells were washed in PBS with 2 mM EDTA and 0.5% bovine serum albumin (BSA) (Carl Roth, Karlsruhe, Germany) and then seeded in RPMI 1640 (Gibco, Darmstadt, Germany) with 1.5% heat-inactivated plasma for 30 min at 37 °C. Non-adherent cells were removed and adherent granulocytes were allowed to detach in the presence of RPMI 1640 with 10% heat-inactivated plasma for 2 h at 37 °C. Afterwards, granulocytes were counted in a haemocytometer using trypan blue exclusion assay to determine cell viability. Cells were seeded at  $1 \times 10^6$  cells/mL in X-Vivo 15 medium (Lonza, Cologne, Germany). The isolation quality was checked by flow cytometry (online suppl. Fig. S1; for all online suppl. material, see [www.karger.com/doi/10.1159/000492678](http://www.karger.com/doi/10.1159/000492678)) using the marker CD15 (for neutrophils and eosinophils) and CD3 (for T cells). The purity was in the range of 80–90%. Only about 3% were phenotyped as CD3+ T cells. Almost all cells proved to be CD15+ when we checked by immunohistochemistry, demonstrating again a high level (>90%) of granulocyte enrichment.

T cells/PBL were isolated from buffy coats by Ficoll-Hypaque density gradient centrifugation. Briefly, 35 mL of blood were pipetted on top of 15 mL of Ficoll (Sigma-Aldrich) in a 50-mL tube and centrifuged for 40 min at 2,500 rpm without brake. A white ring in the middle containing the PBMCs was collected and washed four times in PBS with 2 mM EDTA and 0.5% BSA. The cells were resuspended in RPMI 1640 with 1.5% heat-inactivated plasma and incubated for 30 min at 37 °C in 6-well plates (Corning/Costar, Bodenheim, Germany). Suspension cells were harvested and reseeded in Nunc Easy Flasks (Thermo Scientific, Darmstadt, Germany) for 1 h at 37 °C. Afterwards, the T cells in suspension were carefully removed and seeded at a density of  $1 \times 10^6$  cells/mL in X-Vivo 15 medium for experiments.

### *Blood from Fingertip*

For some immunofluorescence experiments, blood was taken from the fingertip of healthy volunteers using a lancing aid as described [21]. Blood was collected in sodium-heparinised micro-haematocrit glass capillary tubes (Marienfeld Superior, Lauda-Königshofen, Germany). For irradiation experiments, the haematocrit tubes were stored and transported in a 15-mL plastic tube. After treatment, cells were spread onto a glass slide by gentle tapping or flushing the cells out with 5  $\mu$ L of PBS. Samples were air-dried for ~10 min at RT [21]. For staining procedure see further below.

### *Extracellular ROS Detection*

The detection of extracellular ROS has been described elsewhere [9]. Briefly,  $0.5 \times 10^6$  cells were resuspended in 500  $\mu$ L of complete PBS (PBS with 0.5 mM MgCl<sub>2</sub>, 0.7 mM CaCl<sub>2</sub> and 0.1% glucose); 10  $\mu$ g/mL horseradish peroxidase and 10  $\mu$ M luminol were added to the cells before stimulation with 100 ng/mL PMA. The chemiluminescence was measured in a Berthold TriStar<sup>2</sup> LB 942 (Bad Wildbad, Germany) at RT over time.

### *Immunofluorescence Staining of $\gamma$ H2AX, ATM, pATM, pKAP1 and XRCC1*

After treatment, granulocytes and T cells isolated from buffy coats were washed in PBS and centrifuged at 1,500 rpm for 5 min. The supernatant was removed and the cell pellet was taken up in 3  $\mu$ L of PBS. The cell suspension was spread onto a cover slip and the cells were air-dried for a few minutes. Alternatively, blood from the fingertip was collected and blood smears on glass slides were prepared and processed [21]. Cells were permeabilised with methanol:acetone (7:3 ratio) for 6 min at –20 °C. The cover slips were rinsed twice in PBS and then fixed with 2.5% paraformaldehyde for 10 min at RT. Samples were washed with PBS and then blocked in 10% normal goat serum (Invitrogen, Life Technologies) in PBS for 1 h at RT. Cell surface markers CD3 (1477, AbD Serotec MCA, Kidlington, UK) and CD15 (clone HI98, BD Pharmingen, Heidelberg, Germany) were diluted 1:200 in 1% BSA-PBS. The antibodies  $\gamma$ H2AX (phospho Ser139, clone EP854[2]Y; Abcam, Cambridge, UK), pATM (phospho Ser1981, EP1890Y; Abcam), pKAP1 (phospho Ser824; Bethyl Laboratories, Inc.), XRCC1 (EPR4389[2], Abcam) and ATM (D2E2, Cell Signaling Technology, Frankfurt) were diluted 1:1,000 in 1% BSA-PBS and were incubated overnight at 4 °C. The samples were washed 3  $\times$  5 min in PBS, then secondary antibodies were added and incubated for 1 h at RT: goat anti-rabbit Alexa Fluor 488 (Invitrogen, A11070) diluted 1:300 (for detecting  $\gamma$ H2AX, ATM, pATM, pKAP1 and XRCC1) and goat anti-rat Cy3 or goat anti-mouse Cy3 (Jackson ImmunoResearch, West Grove, PA, USA) diluted 1:500 (for detecting CD3 or CD15) in 1% BSA-PBS. The cover slips were washed 3  $\times$  5 min in PBS and stained with 100  $\mu$ M TO-PRO-3 (Invitrogen) for 15 min at RT. The slides were mounted on glass slides using Vectashield medium (Burlingame, CA, USA) and sealed with nail polish. Images were taken using a laser scanning microscope (LSM 710) with the ZEN Software from Carl Zeiss. The signal intensity of the  $\gamma$ H2AX signal in the nucleus was quantified using ImageJ software. The signal intensity was determined by measuring the mean fluorescence of at least 50 cells per experiment. The mean of at least three independent experiments is displayed.

### *Quantification of Cell Death*

Cell death was determined using the trypan blue exclusion assay; 10  $\mu$ L of cell suspension was mixed with 10  $\mu$ L of 0.05% trypan blue in PBS and cells were counted using a haemocytometer. At least 100 cells were counted. Alternatively, cell death was measured by annexin V/PI flow cytometry, which is described in the supplementary material.

### *Neutral, Alkaline and FPG-Modified Alkaline Comet Assays*

DSB formation after IR treatment and single-strand break (SSB) formation after *t*-BOOH treatment were measured using the neutral and the alkaline Comet assay, respectively. After treatment, cells were centrifuged at 1,500 rpm for 5 min at 4 °C. The superna-



tant was discarded, and the cells were resuspended in 0.5% low-melting point agarose and transferred onto agarose-precoated glass slides. For the neutral Comet assay, slides were incubated in cold neutral lysis buffer (10 mM Tris, 2.5 M NaCl, 100 mM EDTA and 1% sodium lauroyl sarcosinate, pH 7.5) for 1 h at 4 °C. Electrophoresis was performed for 22 min at 0.74 V/cm and 300 mA. Afterwards, samples were rinsed with dH<sub>2</sub>O and fixed with ethanol for at least 10 min at –20 °C. For the alkaline Comet assay, slides were incubated in cold alkaline lysis buffer (2.5 M NaCl, 100 mM EDTA, 10 mM Tris, 10% DMSO, 1% Triton X-100, pH 10) for 1 h at 4 °C. DNA unwound in alkaline electrophoresis buffer (300 mM NaOH, 1 mM EDTA, pH >13) for 22 min and electrophoresis was performed for 20 min at 0.74 V/cm and 300 mA. The samples were washed 3 × 5 min in neutralisation buffer (0.4 M Tris, pH 7.5) before they were fixed with 100% ethanol for at least 10 min at –20 °C. For the detection of oxidative DNA lesions, the formamidopyrimidine DNA glycosylase (FPG)-modified alkaline Comet assay was used. Similar to the alkaline Comet assay, cells were incubated in lysis buffer for 1 h at 4 °C. Then, slides were equilibrated 2 × 5 min in buffer F (40 mM HEPES, 0.1 M KCl, 0.5 mM EDTA, 0.2% BSA, pH 8.0) at RT. FPG was diluted in buffer F and 50 µL was added to the slides and incubated in a humid chamber at 37 °C for 45 min. Afterwards, samples were unwound and electrophoresis was performed as in the regular alkaline Comet assay. For all assays, samples were air-dried before the DNA was stained with 50 µg/mL propidium iodide. Comets were analysed by fluorescence microscopy using Olympus BX50 equipped with a ColorView camera (Olympus, Münster, Germany). At least 50 cells were scored in each experiment by means of Comet IV software (Perceptive Instruments Ltd., Bury St. Edmunds, UK). Data were expressed as tail intensity in percent, which represents the percentage of DNA in the tail compared to the total amount of DNA (DNA in head and tail = 100).

#### Protein Expression Analysis by Western Blot

For protein detection, cell pellets were lysed with RIPA buffer (50 mM Tris, 150 mM NaCl, 1 mM EDTA, 1% NP-40, 0.5% sodium deoxycholate, 0.1% SDS, 0.1% sodium azide, 1 mM PMSF, 2 mM sodium orthovanadate, 2 mM DTT and fresh 1× protease inhibitor, pH 8.0). Samples were snap-frozen and thawed on ice twice before they were sonicated with 2 × 5 pulses. Samples were centrifuged at 13,000 g for 10 min at 4 °C. The protein concentration of the supernatant was measured via the Bradford method; 50–100 µg of protein were used for loading. Samples were boiled in loading buffer for 5 min at 56 °C for large proteins (>140 kDa) and at 95 °C for small proteins. SDS-PAGE was performed at 60 V for the stacking gel and increased to 100 V when samples entered the running gel. Proteins were transferred to nitrocellulose membranes at 300 mA for 90 min or at 100 mA overnight at 4 °C. Western blot membranes were blocked in 5% BSA-PBS or 5% dry milk in TBS with 0.1% Tween20. Primary antibodies were diluted 1:1000 and were incubated overnight at 4 °C. The antibodies were as follows: ATM (Cell Signaling Technology), pATM and MGMT (Millipore, Schwalbach, Germany), ATR, XRCC1 and γH2AX (Abcam), GAPDH (Santa Cruz Biotechnology, Heidelberg, Germany), DNA-PK<sub>CS</sub> (Calbiochem, Darmstadt, Germany), PARP-1 (c-IL-10, a kind gift from Prof. A. Bürkle from the University of Konstanz, Germany), ligase III (BD Transduction Laboratories), H2AX (A300–082A, Bethyl Laboratories), p53 (DO-1, Santa Cruz Biotechnology) and p53 Ser15 (Cell Signaling Technology). Sec-

ondary antibodies were IRDye 800CW anti-rabbit and anti-mouse (LI-COR Biosciences, Bad Homburg, Germany) diluted 1:10,000 in Tris-buffered saline with 0.1% Tween20.

#### Statistical Analysis

Results from at least three independent experiments are displayed as  $n \pm$  standard error of mean (SEM). Statistical analysis of data was performed using GraphPad Prism 6 Software.

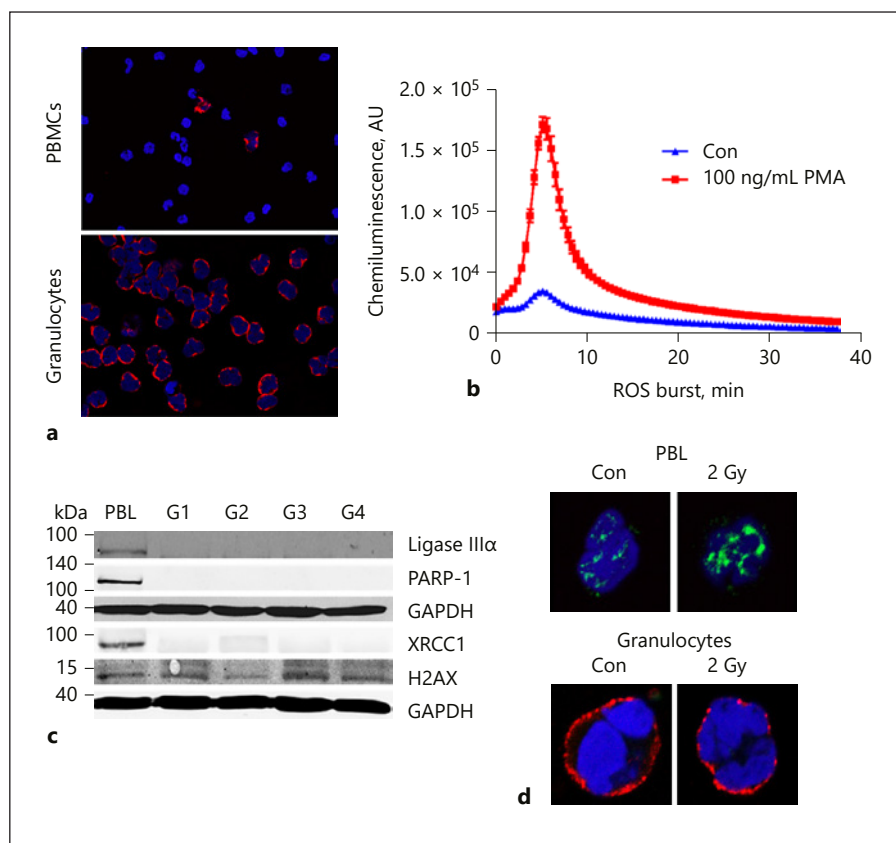
## Results

Granulocytes (containing mostly neutrophils) were isolated from buffy coats of healthy volunteers as described. The purity, controlled by CD15 labelling, was in the range of ~95% (an example is shown in Fig. 1a). The purified granulocytes are biologically active as shown by their response to PMA triggering the ROS burst (Fig. 1b), which is a function of NADPH oxidase [9]. The expression of the BER proteins PARP-1, XRCC1 and ligase IIIα was analysed in Western blots. In comparison to peripheral blood lymphocytes (PBL), none of the granulocyte samples showed the aforementioned proteins (Fig. 1c). In addition, the expression of histone H2AX was measured. H2AX is a target of ATM-mediated phosphorylation (yielding γH2AX), which is triggered after genotoxic insults that result in block of replication and/or DSBs. Histone 2AX was detectable in all granulocyte samples and comparable to the PBL control (Fig. 1c). The expression of these proteins was further measured using a different lysis protocol and other donors, which gave essentially the same results (online suppl. Fig. S2, S3).

To substantiate the data, the expression of XRCC1 was measured via immunofluorescence staining in granulocytes and PBL not treated and treated with γ-rays (2 Gy). XRCC1 was detectable in the nucleus of non-treated PBL (control) and even more pronounced after irradiation, as XRCC1 was recruited to the site of the damage (Fig. 1d). In contrast, granulocytes, which were identified by co-staining with the CD15 surface marker, showed no XRCC1 signal, both in the control and following radiation treatment (Fig. 1d).

Next, we addressed whether the lack of BER proteins had an impact on SSB repair after treatment with the oxidative agent *t*-BOOH. PBL and neutrophilic granulocytes were treated with *t*-BOOH and SSB formation and their subsequent repair were assessed via the alkaline Comet assay. Representative images display strong DNA fragmentation in PBL 30 and 60 min after adding *t*-BOOH (Fig. 2a). Both display high amounts of initial oxidative DNA damage determined 1 h after treatment with

**Fig. 1.** ROS production and BER protein expression in granulocytes obtained from different donors (G1–G4) compared to PBL control. **a** Granulocytes were stained with CD15 and shown to be present in low numbers in the PBMC population (purified by Ficoll gradient centrifugation) and in high numbers in the purified (Optiprep) granulocyte population. Blue staining, nuclei stained with TO-PRO-3; red staining, CD15 surface marker. **b** Extracellular ROS production of granulocytes isolated from buffy coats, which was measured following stimulation with PMA. **c** BER proteins PARP-1, XRCC1 and ligase III $\alpha$  as well as histone 2AX expression, as measured by Western blot experiments. Representative blots are shown. GAPDH, loading control. **d** XRCC1 expression was measured by immunofluorescence staining in PBL and CD15+ granulocytes 1 h after 2-Gy irradiation. Con, control.



100  $\mu$ M *t*-BOOH in the FPG-modified assay (Fig. 2b). Since FPG detects mostly 8-oxo-guanine, the data indicate that similar initial amounts of oxidative DNA lesions were induced in PBL and granulocytes.

Time course experiments revealed that in granulocytes, the *t*-BOOH-induced DNA fragmentation persisted over time. The quantification of DNA fragmentation in the alkaline Comet assay showed that PBL exhibited a massive induction of SSBs after 30 min of treatment. The amount of SSBs dropped rapidly over time but had not reached control level after 6 h (Fig. 2c). Granulocytes, on the other hand, showed reduced SSB formation following *t*-BOOH, which reached its maximum 60 min later and persisted over the following 5 h. The overall SSB level was ~3-fold higher in PBL than in granulocytes. This high SSB level is likely due to incision of DNA during BER, for which granulocytes are impaired.

The induction of cell death after treatment with *t*-BOOH was quantified by trypan blue staining. PBL showed an increase in trypan blue-positive cells in the post-exposure period of 24 h, while granulocytes remained unaffected (Fig. 2d). After 48 h, cell death increased dras-

tically in both control and *t*-BOOH-treated granulocytes with ~60% trypan blue-positive cells in the control and ~80% in the *t*-BOOH-treated population (Fig. 2d). We also determined cell death by annexin V/PI staining, with about 20% apoptosis initially, which raised to about 80% 24 h later (online suppl. Fig. S4). Thus, granulocytes die through apoptosis even in the absence of treatment, supporting the notion that granulocytes do not respond to DNA damage by induction of a cell death programme since they are already primed to undergo death.

Next, we addressed DSB repair in granulocytes. PBL and granulocytes isolated from buffy coats were subjected to Western blot analysis and the DSB repair factors ATM, its phosphorylated form (pATM) and the ATM target H2AX were measured. PBL expressed ATM. After irradiating the cells with 2 Gy, pATM and  $\gamma$ H2AX were detectable. This was not the case in granulocytes, which showed neither basal ATM expression nor phosphorylation of H2AX (Fig. 3a). Lack of ATM in granulocytes was confirmed by immunocytochemistry with ATM staining in PBL, but not in granulocytes (Fig. 3b). The other DNA damage-activated PI3 kinase-related proteins DNA-PK $\text{C}\text{S}$

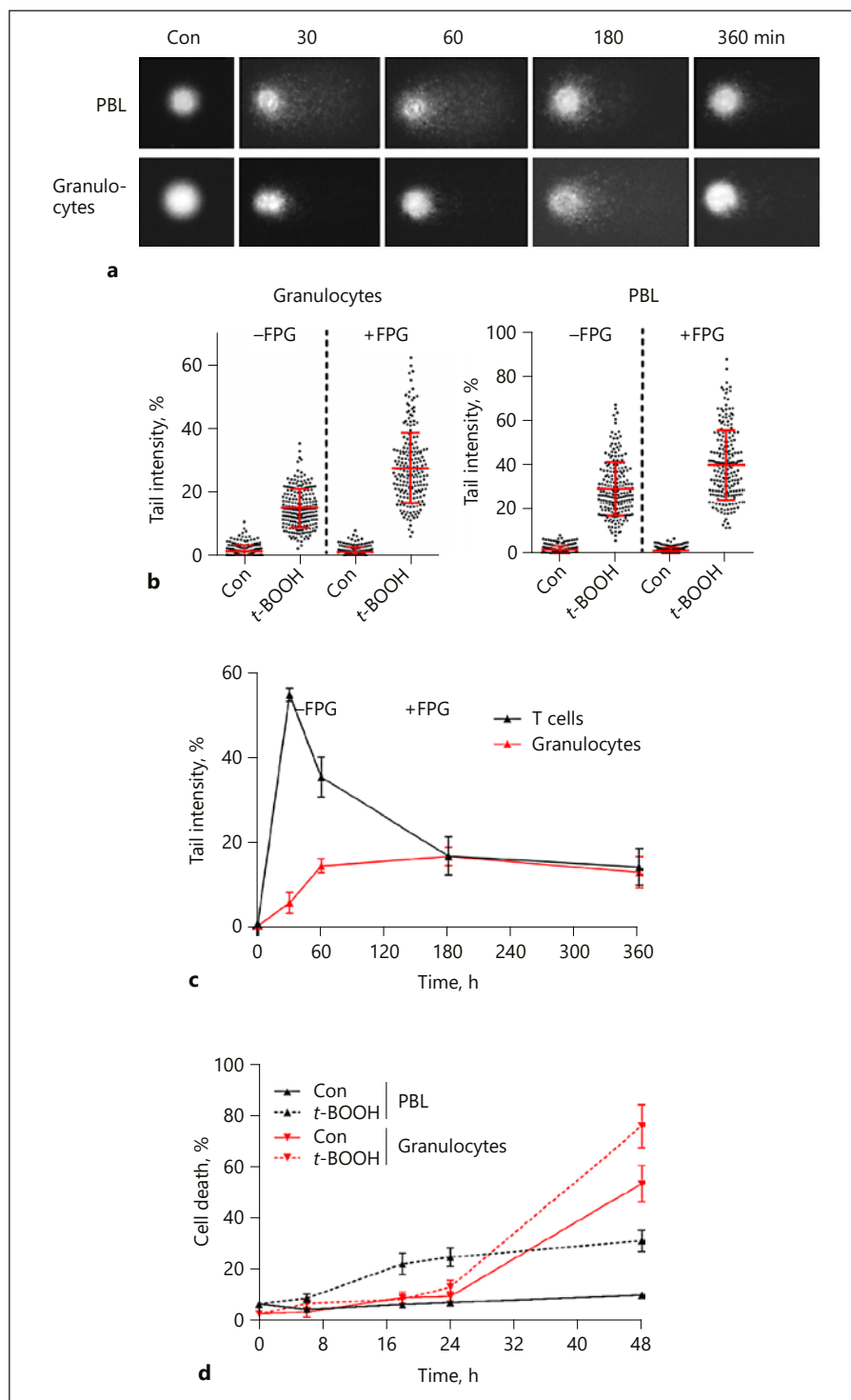


**Fig. 2.** DNA damage and cell death in PBL and granulocytes after treatment with *t*-BOOH. **a** Alkaline Comet assay. Representative images show DNA fragmentation in PBL and granulocytes after treatment with 100  $\mu$ M *t*-BOOH for 30–360 min. **b** The FPG-modified alkaline Comet assay was used to assess the initial oxidative DNA damage in granulocytes and PBL 1 h after treatment with 100  $\mu$ M *t*-BOOH. Cells from the same experiment were analysed by the Comet assay without and with FPG. **c** DNA strand break repair kinetics after treatment of PBL and granulocytes with *t*-BOOH were analysed using the alkaline Comet assay. **d** Cell death of PBL and granulocytes after treatment with *t*-BOOH. Cell death was measured using the trypan blue exclusion assay. Data are the mean  $\pm$  SEM of up to six independent experiments. Con, control.

and ATR were also not detectable in granulocytes (Fig. 3c). In addition, p53 Ser15, which is usually induced following radiation, was measured 1 h after treatment with 2 Gy by immunofluorescence staining and Western blot. Only PBL

showed a signal indicating p53 Ser15 induction, while granulocytes did not respond (online suppl. Fig. S2). Of note, granulocytes did not express the repair protein MGMT (online suppl. Fig. S5). Lack of expression was con-

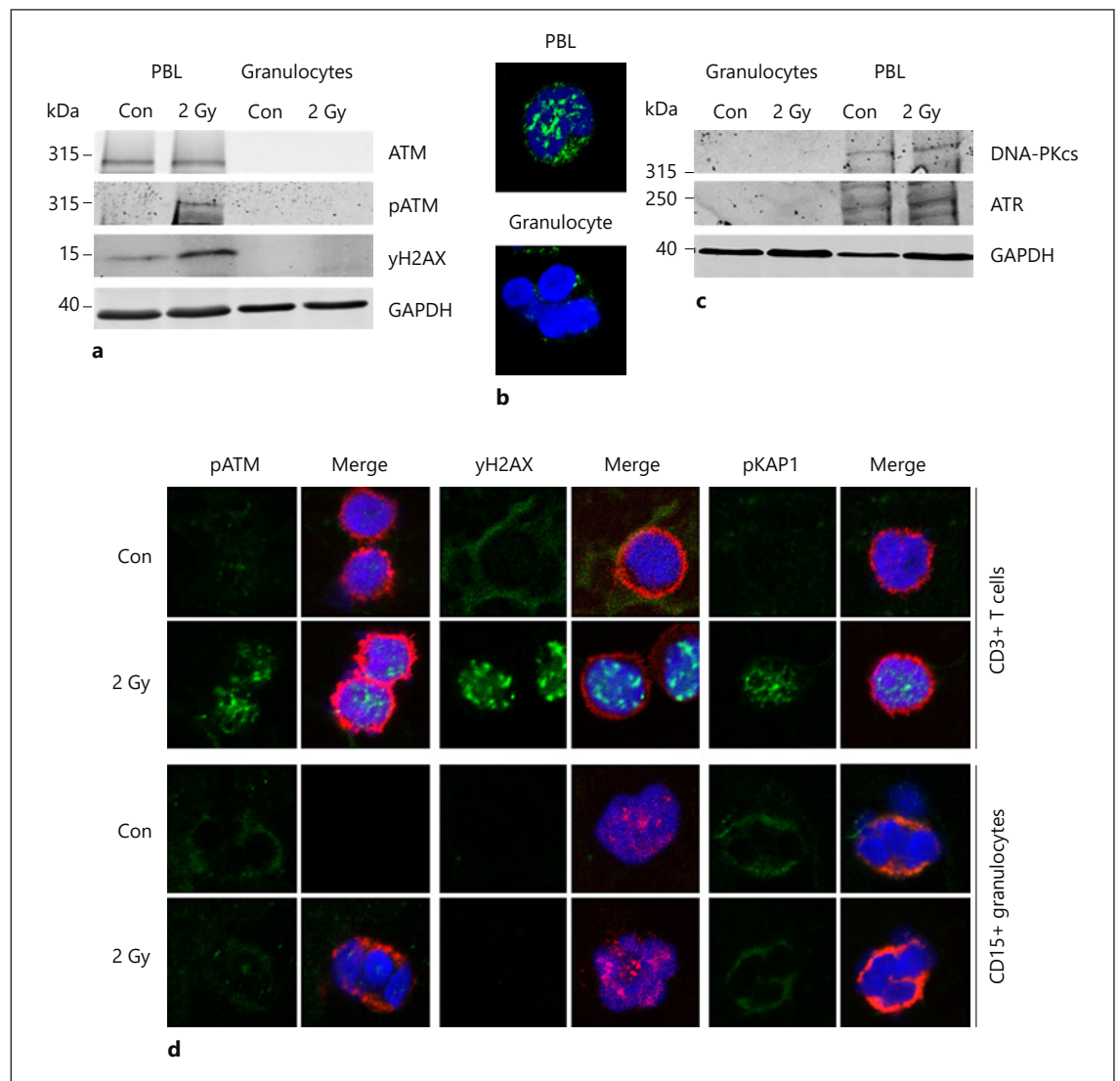


**Fig. 3.** DSB repair protein expression in PBL and granulocytes. **a** Expression of pATM (Ser1981) and phosphorylated histone 2AX (γH2AX) in PBL and granulocytes was measured 1 h after treatment with 2 Gy γ-radiation. **b** Expression of ATM in PBL and granulocytes was determined by immunocytochemistry. Green, ATM; blue, nuclear staining by TO-PRO-3. **c** Expression of DNA-PK<sub>CS</sub> and ATR in PBL and granulocytes was determined 1 h after treatment with 2 Gy. GAPDH served as loading control. **d** pATM

(Ser1981), γH2AX and pKAP1 were analysed in T cells and granulocytes isolated from fresh blood collected from the fingertip of a healthy donor, preserved in micro-haematocrit glass capillary tubes, irradiated and 1 h later immobilised on a glass slide. Red, surface marker CD3+ for T cells and CD15+ for granulocytes; green staining of the corresponding proteins; blue, TO-PRO-3. Representative images are shown. Con, control.

firmed on RNA level where MGMT and ATR transcripts were lacking and ATM and DNA-PK<sub>CS</sub> mRNAs were only weakly expressed compared to PBL (online suppl. Fig. S6).

In the experiments described above, DNA repair protein expression was measured in granulocytes isolated from buffy coats (of healthy volunteers). In order to ensure that the granulocytes were still in prime condition

and not yet aged during granulocyte preparation, fresh blood was collected from the fingertip of healthy volunteers and immediately thereafter treated and immobilised [21]. In brief, a drop of blood from the fingertip was collected in heparinised glass capillaries, and immediately thereafter treated with 2 Gy and incubated for 1 h before it was spread onto glass slides. Cells were co-stained with



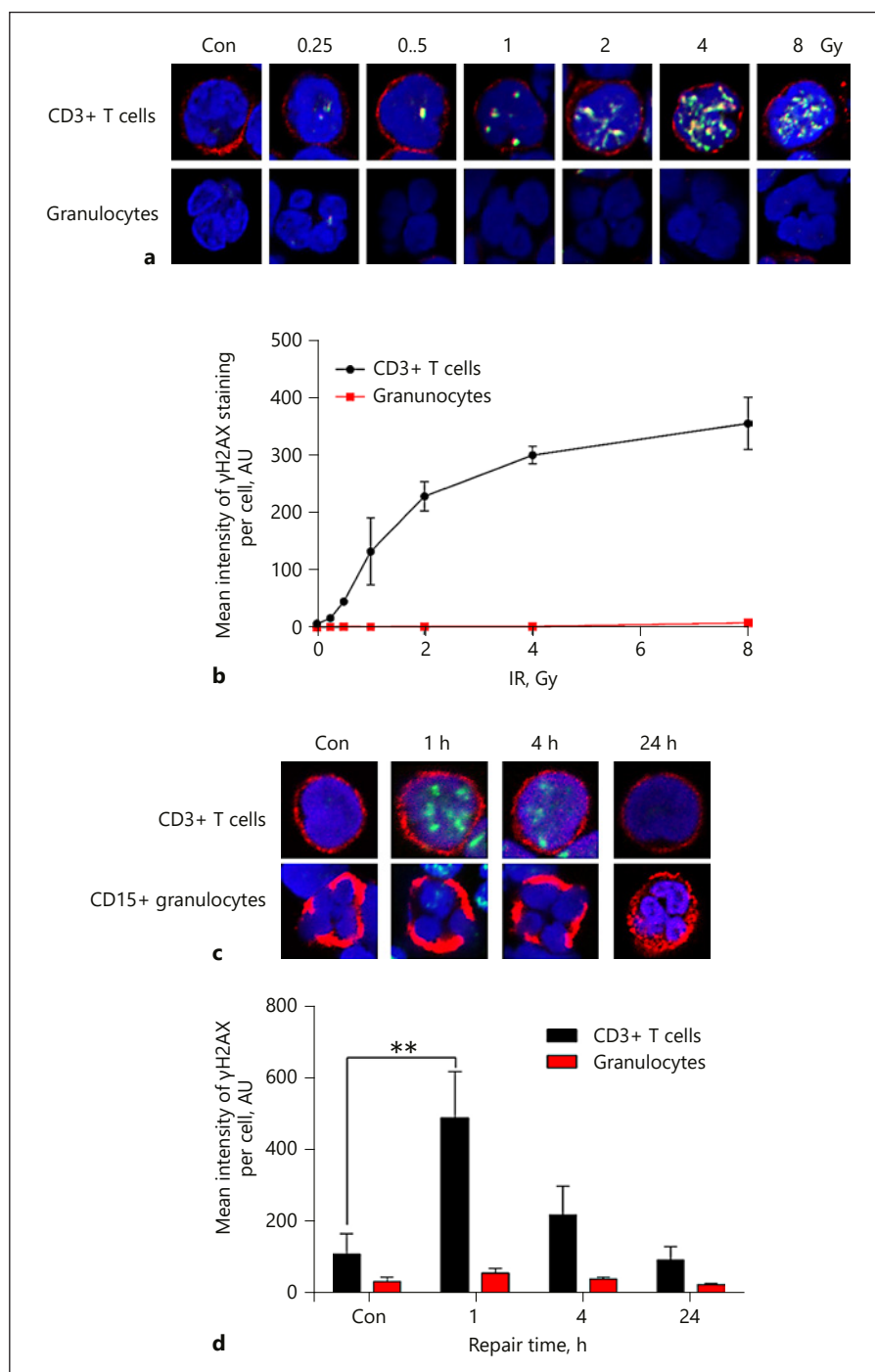


**Fig. 4.** Dose response and repair kinetics of granulocytes and CD3+ T cells after treatment with ionising radiation. **a**  $\gamma$ H2AX foci staining in CD3+ T cells and granulocytes was measured 1 h after treatment with increasing doses of  $\gamma$ -rays. T cells were labelled with CD3 (red). Purified granulocytes display the typical segmented nucleus. **b** Quantification of  $\gamma$ H2AX signal intensity. Granulocytes did not display any discernible  $\gamma$ H2AX signal. Data are the mean  $\pm$  SEM of three independent experiments with at least 50 cells counted. **c**  $\gamma$ H2AX was measured over time in CD3+ T cells and CD15+ granulocytes after 2 Gy irradiation. Representative images are shown. Green,  $\gamma$ H2AX; red, CD3 or CD15 for T cells and granulocytes, respectively. **d** Quantification of the  $\gamma$ H2AX signal in T cells and granulocytes 1, 4 and 24 h after radiation treatment. Data are the mean  $\pm$  SEM of four independent experiments with at least 50 cells counted. \*\*  $p < 0.001$ , 2-way ANOVA, Tukey's multiple comparison test. Con, control.

CD3 for detecting T cells and CD15 for granulocytes. CD3+ T cells (red ring) were positive for pATM,  $\gamma$ H2AX and pKAP1 after 2 Gy irradiation (Fig. 3d, upper panel) while CD15+ granulocytes showed no signal in the immunofluorescence images (Fig. 3d, lower panel). This data confirmed what we observed in the Western blot analysis.

A target of ATM is KAP-1, which is a transcriptional repressor that mediates gene silencing by increasing the amount of histone 3 methylated lysine 9 (H3K9me). It is also involved in the degradation of p53 [22, 23]. Interestingly, pKAP1 was also not detectable (Fig. 3d), confirming a lack of ATM protein and ATM activity in granulocytes.



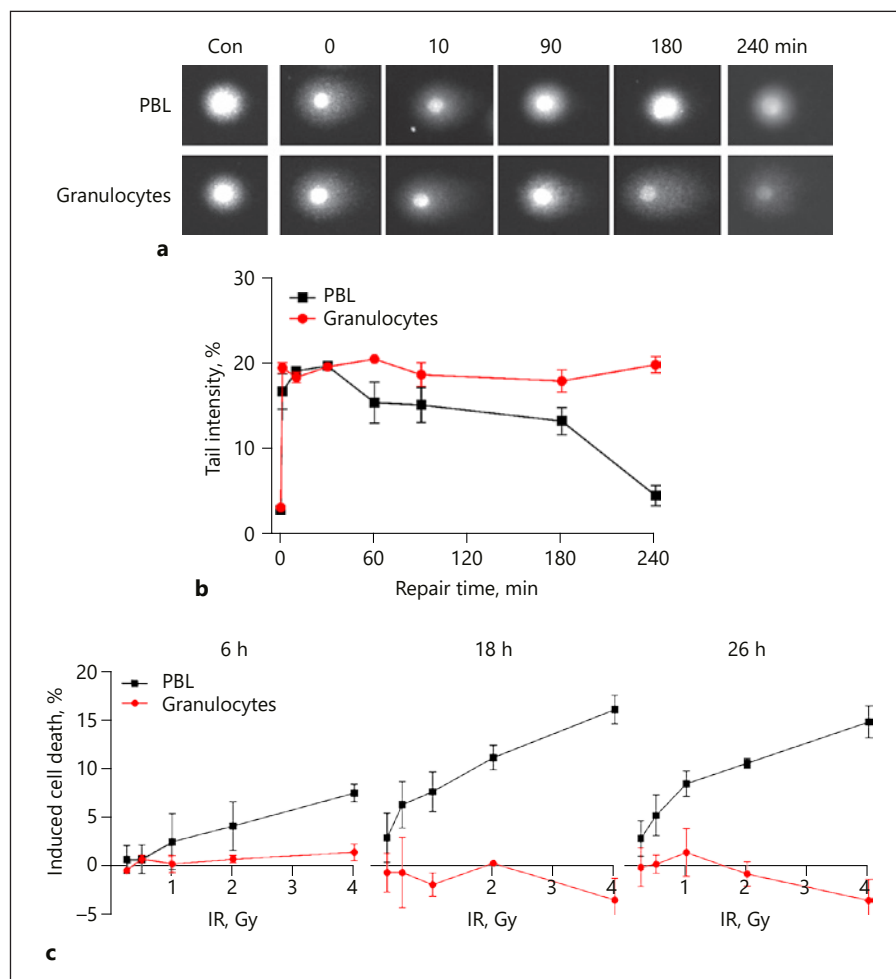


**Fig. 5.** DNA double-strand break repair and cell death in T cells and granulocytes after ionising radiation. **a** Representative images of cells processed by the neutral Comet assay. Con, control. **b** Quantification of the DSB formation in PBL and granulocytes measured by the neutral Comet assay. **c** Cell death was measured 6, 18 and 24 h after treating the cells with IR in a dose range from 0.25 to 4 Gy. Cell death was quantified by trypan blue exclusion. Data are the mean  $\pm$  SEM of three independent experiments.

As  $\gamma$ H2AX was not detectable in granulocytes irradiated with 2 Gy (1 h post-incubation), we were interested to assess whether higher doses of IR led to detectable  $\gamma$ H2AX. CD3<sup>+</sup> T cells and granulocytes obtained from buffy coats were treated with IR ranging from 0.25 to 8 Gy and incubated for 1 h. Representative images showed a dose-dependent increase in  $\gamma$ H2AX signals in the CD3<sup>+</sup> T cells (red ring), whereas granulocytes showed no discernible signal (Fig. 4a). In contrast, PBL proved to be very sensitive to low doses of IR and showed a linear increase in their  $\gamma$ H2AX signal intensity in the range of 0.25–2 Gy (Fig. 4b). Saturation levels in the  $\gamma$ H2AX signal were observed at higher doses, i.e. 4 and 8 Gy. Granulocytes, on the other hand, showed no discernible  $\gamma$ H2AX signal, neither as pan-staining nor as foci, at all dose levels tested (Fig. 4a, b).

In addition to the dose-response, time course experiments were performed. CD3<sup>+</sup> T cells and granulocytes were treated with 2 Gy and  $\gamma$ H2AX was detected through immunofluorescence staining 1, 4 and 24 h after treat-

ment. Representative images (Fig. 4c) and the quantification of the mean fluorescence intensity of the  $\gamma$ H2AX signal (Fig. 4d) showed a peak of the  $\gamma$ H2AX signal after 1 h that dropped to control level within 24 h in CD3<sup>+</sup> T cells, indicating that repair of DSBs was successfully performed. In contrast, granulocytes showed no  $\gamma$ H2AX signal immediately after irradiation and during the post-incubation period, indicating that they are strongly impaired in executing DDR.

Next, we analysed whether the absence of DDR signalling had an impact on the repair of DSBs in granulocytes. As control we again used PBL. These cells (from the same donor) and granulocytes were irradiated with 2 Gy and the DSB formation and their subsequent repair were analysed by the neutral Comet assay. Representative Comet tail images showed strong DNA fragmentation immediately after IR treatment (zero time; Fig. 5a) in both populations. However, in granulocytes the DNA tail persisted over the observation period of 4 h, whereas in PBL the DNA fragmen-

tation induced by IR declined to almost control level (Fig. 5b; online suppl. Fig. S7). The data imply successful DSB repair to occur in PBL, but not in granulocytes.

In view of the lack of DDR in granulocytes, the question arises as to whether granulocytes undergo cell death following IR. Radiation-induced death of granulocytes was analysed by trypan blue exclusion 6, 18 and 24 h after treatment. PBL displayed a dose- and time-dependent increase in radiation-induced trypan blue-positive cells. Thus, 6 h after treatment, only a marginal increase in dead cells was observed, whereas after 18 and 24 h radiation-induced death significantly increased in PBL (Fig. 5c). Granulocytes, on the other hand, did not display radiation-induced cell death (Fig. 5c). Of note, at later times granulocytes showed a spontaneous time-dependent increase in cell death (see Fig. 2d for experiments with *t*-BOOH and online suppl. Fig. S8 for IR), which was, however, independent of DNA damaging treatment.

## Discussion

Human neutrophilic granulocytes are crucial in the innate immune response. Following release from the bone marrow, they are rapidly recruited to the site of inflammation where they kill invading pathogens through the release of ROS and phagocytosis [24, 25]. Their importance is exemplified in patients suffering from neutropenia, chronic granulomatous disease and leukocyte adhesion deficiency, who are prone to recurring severe bacterial and fungal infections. Neutrophils are the most abundant leukocyte cell type, characterised by a short circulating half-life and a high basal production level [26]. Our previous work with monocytes and monocyte-derived macrophages and DC revealed a marked difference in the expression of DNA repair proteins with an impact on their DNA repair capacity. Monocytes are impaired in base excision and SSB repair as they do not or only weakly express a couple of key repair proteins such as XRCC1, PARP-1, ligase III $\alpha$  and DNA-PK $\text{CS}$ . This repair deficiency makes them sensitive to genotoxic treatments. Thus, oxidising agents (e.g. *t*-BOOH,  $\text{H}_2\text{O}_2$  and their own ROS burst), oxidated low-density lipoprotein (oxLDL), methylating agents (MNNG, MMS and temozolomide) and ionising radiation gave rise to accumulation of DNA damage and subsequent monocyte cell death. Differentiation of monocytes into macrophages and DC, mediated by GM-CSF and GM-CSF + IL-4, respectively, results in re-expression of the DNA repair proteins and consequently genotoxin resistance, including resistance

to IR and chemical ROS, due to successful DNA repair [13–15].

Granulocytes arise from the same precursor as monocytes and, therefore, belong to the same myeloid lineage [1]. Although neutrophils represent the most abundant granulocyte and leukocyte population, there are only limited studies as to their DNA repair capacity. Thus, gene expression screening provided data to indicate that CD16+ neutrophils are defective in SSB and DSB repair whereas CD16+ eosinophils remained repair efficient [27]. There is a report demonstrating that neutrophils isolated from peripheral blood lacked DNA-PK and PARP-1, but expressed Ku70 and Ku86 [28]. It was also reported that PMA-treated blood cells displayed phosphorylation of ATM and H2AX in granulocytes, monocytes and lymphocytes [29]. Another study found phosphorylated ATM and H2AX ( $\gamma\text{H2AX}$ ) in neutrophils after NADPH oxidase activation and IR [30]. In view of these rather controversial results we analysed DNA repair protein expression and DNA repair capacity in granulocytes after exposure to ROS and IR. The granulocyte population isolated by us consisted mostly of neutrophils (>80%). Similar to monocytes, neutrophils displayed severe DNA repair defects. Using immunofluorescence staining and Western blot analysis, we show that BER, alternative NHEJ and SSB repair were affected, which require PARP-1, XRCC1 and ligase III $\alpha$  that were not expressed in neutrophils. For confirmation of Western blots, an alternative protocol for lysing the cells was used [28], including a mixture of PBL and neutrophils (2:1 in order to check degradation of proteins through the neutrophil extract) and subjected to SDS-PAGE and Western blot analysis. We consistently observed in these experiments that neutrophils did not express PARP-1 and XRCC1. Of note, p53 was also not detectable following IR treatment in these granulocytes harvested from peripheral blood.

The lack of repair proteins resulted in persisting DNA damage when cells were treated with the oxidising agent *t*-BOOH. Thus, while in PBL massive SSB formation was observed, which rapidly declined over a period of 6 h, in neutrophils the SSB formation was weaker, likely due to the lack of SSB intermediates resulting from BER. However, the generated SSBs persisted over the observed time period, indicating impaired SSB repair.

The DSB repair defect of neutrophilic granulocytes was even more severe than that observed previously in monocytes [14]. Both cell types lacked DNA-PK $\text{CS}$  protein expression; however, unlike in monocytes the DNA damage response kinases ATR and ATM were also not detectable in neutrophilic granulocytes. This contrasts

with a previous report where ATM was activated and pATM was detected after IR or PMA treatment [30]. Furthermore, the DSB marker  $\gamma$ H2AX was also not detectable in dose- and time-response experiments after treatment with IR, which is compatible with the observed lack of DNA damage-dependent kinases in our samples. The resulting DSBs remained unrepaired in neutrophils, whereas in PBL a reduction in DSBs was visible in the neutral Comet assay after 6 h, implying successful DSB repair in PBL, but not in neutrophilic granulocytes.

Interestingly, the trypan blue exclusion experiments showed only a small effect of *t*-BOOH and radiation on neutrophil cell death. We should note that the basal cell death rate (trypan blue-positive cells) was increasing with time in culture in the absence of genotoxic treatment in the 48-h cultivation period, which is in line with a reported lifespan of 1–2 days and the extremely high turnover rate [31]. PBL, on the other hand, showed a significant increase in the rate of induced death following genotoxic treatment. We conclude that terminally differentiated neutrophilic granulocytes in the peripheral blood are primed to undergo spontaneous cell death and are unable to activate the DNA damage-triggered cell death cascade.

The unique phenotype of neutrophils in the peripheral blood, being unable to repair their DNA and activate the DNA damage response pathway, may be explained by their biological destination. Unlike monocytes, which differentiate into long-living macrophages and DC, neutrophils are terminally differentiated with a short lifespan. They are constantly produced and released from the bone marrow into the bloodstream and recruited to the site of infection. Upon activation, they respond with a burst of ROS in amounts high enough to produce DNA damage in cells in their vicinity and killing them, which was demonstrated for monocytes and T cells [9]. As shown for activated monocytes and macrophages [9], their ROS burst very likely causes severe oxidative damage to their own DNA, which needs to be repaired in order to maintain proper cellular functions. However, DNA repair is an energy-consuming process (see ATP depletion following PARP-1 activation) and, therefore, it is reasonable to speculate that DNA repair in activated, self-damaged neutrophils would be detrimental to the organism. Also, DNA repair in terminally differentiated neutrophils seems not to be necessary for ensuring their function in the innate immune response. One may even speculate that the vast downregulation of DNA repair functions helps neutrophils to undergo death following release into the bloodstream and recruitment to the site of infection, supporting mechanistically their extremely high turnover rate. In ad-

dition, it is conceivable that DNA repair is counterproductive regarding the process of NET formation, which rests on the release of neutrophil's nuclear DNA into the extracellular space. One may speculate that DNA containing nicks or oxidative DNA damage is more efficient in forming NETs than unbroken (high-molecular weight) DNA and, therefore, DNA breaks due to failure in DNA repair are of advantage in this process, but this needs to be proven. It is striking that all cell types in the haematopoietic system are DSB repair competent [16], except monocytes [14] and, as shown here, terminally differentiated neutrophils in the peripheral blood. This raises the question as to the mechanism of downregulation of these DNA repair genes. *As granulocytes arise from the same precursor as monocytes and both share the same unique, DNA repair-impaired phenotype, it is conceivable that downregulation of DNA repair occurs at the precursor stage, which is currently under investigation.*

Regarding the induced cytotoxicity, we should also note that granulocytes show a clearly higher death rate than PBL in vitro, resulting from their endogenous death programme. This is in line with data in the literature, reporting a lifespan range from 8 h to 5.4 days [1]. In view of the high spontaneous death level, it is difficult to assess the contribution of external genotoxic stress, which can be observed in T cells and other haematopoietic cell types that have a much longer lifespan. Therefore, we do not state that granulocytes are hypersensitive to genotoxins regarding killing effects. Our main conclusion is that they are defective in DNA repair and many components of DNA damage signalling. It is reasonable to speculate that downregulation of DNA repair/DDR is of biological significance as granulocytes do not need an intact genome anymore and DNA repair might even be hindering some of their functions such as NET formation. Thus, in view of the short lifespan of granulocytes in the peripheral blood it is conceivable that DNA repair is not needed anymore. For the different subpopulations of T cells, we have data at hand to show that they are quite radiation sensitive, responding in a similar way to IR, although regulatory T cells exhibit a specific sensitivity to cyclophosphamide [32]. Although terminally differentiated, T cell populations have quite a long lifespan and, therefore, they obviously need DNA repair in order to survive, given the 40,000 DNA lesions induced per genome per day spontaneously [33]. The massive downregulation of DNA repair in terminally differentiated neutrophils provides an example of intense regulation of DNA repair in biological systems that, similar to what we postulated for monocytes [9], very likely plays a biological role in blood homeostasis.

## Acknowledgements

We gratefully acknowledge Prof. Walter Hitzler and Dr. Roland Conradi for their cooperation and generous supply of buffy coats. This work was supported by Deutsche Forschungsgemeinschaft (DFG-KA724/20-2).

## Disclosure Statement

The authors declare that they have no conflicting interests.

## References

- Kolaczowska E, Kubes P. Neutrophil recruitment and function in health and inflammation. *Nat Rev Immunol*. 2013 Mar;13(3):159–75.
- Buvelot H, Posfay-Barbe KM, Linder P, Schrenzel J, Krause KH. Staphylococcus aureus, phagocyte NADPH oxidase and chronic granulomatous disease. *FEMS Microbiol Rev*. 2017 Mar;41(2):139–57.
- Strydom N, Rankin SM. Regulation of circulating neutrophil numbers under homeostasis and in disease. *J Innate Immun*. 2013;5(4):304–14.
- Hoenderdos K, Condliffe A. The neutrophil in chronic obstructive pulmonary disease. *Am J Respir Cell Mol Biol*. 2013 May;48(5):531–9.
- Kaplan MJ. Role of neutrophils in systemic autoimmune diseases. *Arthritis Res Ther*. 2013 Oct;15(5):219.
- Bedard K, Krause KH. The NOX family of ROS-generating NADPH oxidases: physiology and pathophysiology. *Physiol Rev*. 2007 Jan;87(1):245–313.
- Nandoskar M, Ferrante A, Bates EJ, Hurst N, Paton JC. Inhibition of human monocyte respiratory burst, degranulation, phospholipid methylation and bactericidal activity by pneumolysin. *Immunology*. 1986 Dec;59(4):515–20.
- Slauch JM. How does the oxidative burst of macrophages kill bacteria? Still an open question. *Mol Microbiol*. 2011 May;80(3):580–3.
- Ponath V, Kaina B. Death of Monocytes through Oxidative Burst of Macrophages and Neutrophils: killing in Trans. *PLoS One*. 2017 Jan;12(1):e0170347.
- Khandpur R, Carmona-Rivera C, Vivekanandan-Giri A, Gizinski A, Yalavarthi S, Knight JS, et al. NETs are a source of citrullinated autoantigens and stimulate inflammatory responses in rheumatoid arthritis. *Sci Transl Med*. 2013 Mar;5(178):178ra40.
- Yipp BG, Kubes P. NETosis: how vital is it? *Blood*. 2013 Oct;122(16):2784–94.
- Lee KH, Kronbichler A, Park DD, Park Y, Moon H, Kim H, et al. Neutrophil extracellular traps (NETs) in autoimmune diseases: A comprehensive review. *Autoimmun Rev*. 2017 Nov;16(11):1160–73.
- Briegert M, Kaina B. Human monocytes, but not dendritic cells derived from them, are defective in base excision repair and hypersensitive to methylating agents. *Cancer Res*. 2007 Jan;67(1):26–31.
- Bauer M, Goldstein M, Christmann M, Becker H, Heylmann D, Kaina B. Human monocytes are severely impaired in base and DNA double-strand break repair that renders them vulnerable to oxidative stress. *Proc Natl Acad Sci USA*. 2011 Dec;108(52):21105–10.
- Bauer M, Goldstein M, Heylmann D, Kaina B. Human monocytes undergo excessive apoptosis following temozolomide activating the ATM/ATR pathway while dendritic cells and macrophages are resistant. *PLoS One*. 2012;7(6):e39956.
- Heylmann D, Rödel F, Kindler T, Kaina B. Radiation sensitivity of human and murine peripheral blood lymphocytes, stem and progenitor cells. *Biochim Biophys Acta*. 2014 Aug;1846(1):121–9.
- Audebert M, Salles B, Calsou P. Involvement of poly(ADP-ribose) polymerase-1 and XRCC1/DNA ligase III in an alternative route for DNA double-strand breaks rejoining. *J Biol Chem*. 2004 Dec;279(53):55117–26.
- Caldecott KW. XRCC1 and DNA strand break repair. *DNA Repair (Amst)*. 2003 Sep;2(9):955–69.
- Matsuoka S, Ballif BA, Smogorzewska A, McDonald ER 3rd, Hurov KE, Luo J, et al. ATM and ATR substrate analysis reveals extensive protein networks responsive to DNA damage. *Science*. 2007 May;316(5828):1160–6.
- Roos WP, Thomas AD, Kaina B. DNA damage and the balance between survival and death in cancer biology. *Nat Rev Cancer*. 2016 Jan;16(1):20–33.
- Heylmann D, Kaina B. The  $\gamma$ H2AX DNA damage assay from a drop of blood. *Sci Rep*. 2016 Mar;6(1):22682.
- Wang C, Ivanov A, Chen L, Fredericks WJ, Seto E, Rauscher FJ 3rd, et al. MDM2 interaction with nuclear corepressor KAP1 contributes to p53 inactivation. *EMBO J*. 2005 Sep;24(18):3279–90.
- White D, Rafalska-Metcalf IU, Ivanov AV, Corsinotti A, Peng H, Lee SC, et al. The ATM substrate KAP1 controls DNA repair in heterochromatin: regulation by HP1 proteins and serine 473/824 phosphorylation. *Mol Cancer Res*. 2012 Mar;10(3):401–14.
- Amulic B, Cazalet C, Hayes GL, Metzler KD, Zychlinsky A. Neutrophil function: from mechanisms to disease. *Annu Rev Immunol*. 2012;30(1):459–89.
- El Kebir D, Filep JG. Role of neutrophil apoptosis in the resolution of inflammation. *Sci World J*. 2010 Sep;10:1731–48.
- Summers C, Rankin SM, Condliffe AM, Singh N, Peters AM, Chilvers ER. Neutrophil kinetics in health and disease. *Trends Immunol*. 2010 Aug;31(8):318–24.
- Salati S, Bianchi E, Zini R, Tenedini E, Quaglino D, Manfredini R, et al. Eosinophils, but not neutrophils, exhibit an efficient DNA repair machinery and high nucleolar activity. *Haematologica*. 2007 Oct;92(10):1311–8.
- Kurosawa A, Shinohara K, Watanabe F, Shimizu-Saito K, Koiwai O, Yamamoto K, et al. Human neutrophils isolated from peripheral blood contain Ku protein but not DNA-dependent protein kinase. *Int J Biochem Cell Biol*. 2003 Jan;35(1):86–94.
- Tanaka T, Halicka HD, Traganos F, Darzynkiewicz Z. Phosphorylation of histone H2AX on Ser 139 and activation of ATM during oxidative burst in phorbol ester-treated human leukocytes. *Cell Cycle*. 2006 Nov;5(22):2671–5.
- Harbort CJ, Soeiro-Pereira PV, von Bernuth H, Kaindl AM, Costa-Carvalho BT, Condino-Neto A, et al. Neutrophil oxidative burst activates ATM to regulate cytokine production and apoptosis. *Blood*. 2015 Dec;126(26):2842–51.
- Dancey JT, Deubelbeiss KA, Harker LA, Finch CA. Neutrophil kinetics in man. *J Clin Invest*. 1976 Sep;58(3):705–15.
- Heylmann D, Bauer M, Becker H, van Gool S, Bacher N, Steinbrink K, et al. Human CD4+CD25+ regulatory T cells are sensitive to low dose cyclophosphamide: implications for the immune response. *PLoS One*. 2013 Dec;8(12):e83384.
- Lindahl T. Instability and decay of the primary structure of DNA. *Nature*. 1993 Apr;362(6422):709–15.